Unified character of correlation effects in unconventional Pu-based superconductors and δ-Pu

A. B. Shick,[1,2] J. Kolorenc,[2] J. Rusz,[3,2] P. M. Oppeneer,[3]
A. I. Lichtenstein,[4] M. I. Katsnelson,[5] and R. Caciuffo[1]

[1] *European Commission, Joint Research Centre, Institute for Transuranium Elements, Postfach 2340, D-76125 Karlsruhe, Germany*
[2] *Institute of Physics, ASCR, Na Slovance 2, CZ-18221 Prague, Czech Republic*
[3] *Dept. of Physics and Astronomy, Uppsala University, Box 516, S-751 20 Uppsala, Sweden*
[4] *University of Hamburg, Jungiusstrasse 9, 20355 Hamburg, Germany*
[5] *Radboud University Nijmegen, Heyendaalseweg 135, 6525 AJ Nijmegen, The Netherlands*

(Dated: January 17, 2013)

Electronic structure calculations combining the local-density approximation with an exact diagonalization of the Anderson impurity model show an intermediate $5f^5$-$5f^6$-valence ground state and delocalization of the $5f^5$ multiplet of the Pu atom $5f$-shell in $PuCoIn_5$, $PuCoGa_5$, and δ-Pu. The $5f$-local magnetic moment is compensated by a moment formed in the surrounding cloud of conduction electrons. For $PuCoGa_5$ and δ-Pu the compensation is complete and the Anderson impurity ground state is a singlet. For $PuCoIn_5$ the compensation is partial and the Pu ground state is magnetic. We suggest that the unconventional d-wave superconductivity is likely mediated by the $5f$-states antiferromagnetic fluctuations in $PuCoIn_5$, and by valence fluctuations in $PuCoGa_5$.

PACS numbers: 74.70.Tx, 74.45.+c, 74.20.Mn, 74.20.Pq

Providing a consistent description of correlation effects in the electronic structure of elemental actinides and their compounds is a complex problem due to the interplay between the localized and the itinerant nature of the 5f electrons. It is commonly accepted that $5f$-electrons in light actinides form rather broad conduction bands whereas for the heavy actinides the $5f$ states are atomic-like. Johansson [1] described this situation as a "Mott transition in the $5f$-electron subsystem" taking place between Pu and Am when moving along the Periodic Table. Katsnelson *et al.* [2] linked the broadening of the $5f$ band to the "atomic collapse" characterizing the transformation from the high-temperature expanded and the low-temperature compressed phases of Pu.

A quantitative description of the Mott transition in actinides [3] was obtained by the dynamical mean-field theory (DMFT) [4] more than 20 years after the concept was formulated. Further DMFT studies suggested an intermediate-valence nature of the Pu-atom $5f$ shell [5] and provided justification for the experimentally proved absence of magnetism in δ-Pu [6].

The intermediate-valence and nonmagnetic character of the $5f$ shell can play an important role in stabilizing the superconducting state exhibited by $PuCoGa_5$ below a critical temperature T_c of 18.5 K. [7–9]. The unconventional character of superconductivity in this compound is now generally accepted but the microscopic mechanism responsible for electron pairing remains unknown. The d-wave symmetry of the superconducting gap in $PuCoGa_5$ has been proven by point-contact spectroscopy experiments [10] that also provided the first spectroscopic measurements of the gap amplitude and its temperature dependence.

Recently, superconductivity has been discovered also in $PuCoIn_5$ [11], with $T_c = 2.5$ K. The experimental studies of this compound were immediately followed by conventional density functional theory (DFT) calculations in the local-density generalized-gradient approximation (LDA/GGA) [12, 13]. Keeping in mind a well known failure of DFT in the case of δ-Pu [6], it can be expected that LDA/GGA does not provide an accurate description of the electronic structure for this strongly correlated material. A few static mean-field correlated band theory calculations were also performed [12, 14], making use of different flavors of the LDA/GGA plus Coulomb's U (LDA+U) method. While being an improvement over the conventional band theory, the LDA(GGA)+U falls short in describing the itinerant-to-localized crossover of the $5f$ manifold in δ-Pu [5] and $PuCoGa_5$ [10].

Here, we report electronic structure calculations of $PuCoIn_5$, $PuCoGa_5$ and δ-Pu performed by combining LDA with the exact diagonalization (ED) [15] of a discretized single-impurity Anderson model [16]. In this approach, the band structure obtained by the relativistic version of the full-potential linearized augmented plane wave method (FP-LAPW) [17] is consistently extended to account for the full structure of the $5f$-orbital atomic multiplets and their hybridization with the conduction bands [18].

The starting point of our approach is the multiband Hubbard Hamiltonian [19] $H = H^0 + H^{\rm int}$. $H^0 = \sum_{i,j,\gamma} H^0_{i\gamma_1,j\gamma_2} c^\dagger_{i\gamma_1} c_{j\gamma_2}$, where i,j label lattice sites and $\gamma = (lm\sigma)$ mark spinorbitals $\{\phi_\gamma\}$, is the

one-particle Hamiltonian found from *ab initio* electronic structure calculations of a periodic crystal; $H^{\rm int}$ is the on-site Coulomb interaction [19] describing the f-electron correlation. We assume that electron interactions in the s, p, and d shells are well approximated in DFT.

The effects of the interaction Hamiltonian $H^{\rm int}$ on the electronic structure are described by a **k**-independent one-particle selfenergy $\Sigma(z)$, where z is a (complex) energy. The selfenergy is constructed with the aid of an auxiliary impurity model describing the complete seven-orbital $5f$ shell. This multi-orbital impurity model includes the full spherically symmetric Coulomb interaction, the spin-orbit coupling (SOC), and the crystal field (CF). The corresponding Hamiltonian can be written as [16]

$$\begin{aligned} H_{\rm imp} = & \sum_{\substack{kmm'\\ \sigma\sigma'}} [\epsilon^k]^{\sigma\ \sigma'}_{mm'} b^\dagger_{km\sigma} b_{km'\sigma'} + \sum_{m\sigma} \epsilon_f f^\dagger_{m\sigma} f_{m\sigma} \\ & + \sum_{mm'\sigma\sigma'} \left[\xi \mathbf{l}\cdot\mathbf{s} + \Delta_{\rm CF}\right]^{\sigma\ \sigma'}_{mm'} f^\dagger_{m\sigma} f_{m'\sigma'} \\ & + \sum_{\substack{kmm'\\ \sigma\sigma'}} \left([V^k]^{\sigma\ \sigma'}_{mm'} f^\dagger_{m\sigma} b_{km'\sigma'} + \text{h.c.} \right) \\ & + \frac{1}{2} \sum_{\substack{mm'm''\\ m'''\sigma\sigma'}} U_{mm'm''m'''} f^\dagger_{m\sigma} f^\dagger_{m'\sigma'} f_{m'''\sigma'} f_{m''\sigma}, \end{aligned} \tag{1}$$

where $f^\dagger_{m\sigma}$ creates an electron in the $5f$ shell and $b^\dagger_{m\sigma}$ creates an electron in the "bath" that consists of those host-band states that hybridize with the impurity $5f$ shell. The energy position ϵ_f of the impurity level, and the bath energies ϵ^k are measured from the chemical potential μ. The parameter ξ specifies the strength of the SOC and $\Delta_{\rm CF}$ is the crystal-field potential at the impurity. The parameter matrices V^k describe the hybridization between the $5f$ states and the bath orbitals at energy ϵ^k.

The band Lanczos method [15] is employed to find the lowest-lying eigenstates of the many-body Hamiltonian $H_{\rm imp}$ and to calculate the one-particle Green's function $[G_{\rm imp}(z)]^{\sigma\ \sigma'}_{mm'}$ in the subspace of the f orbitals at low temperature ($k_{\rm B}T = 1/500$ eV). The self-energy $[\Sigma(z)]^{\sigma\ \sigma'}_{mm'}$ is then obtained from the inverse of the Green's-function matrix $[G_{\rm imp}]$.

Once the self-energy is known, the local Green's function $G(z)$ for the electrons in the solid,

$$[G(z)]_{\gamma_1\gamma_2} = \frac{1}{V_{\rm BZ}} \int_{\rm BZ} {\rm d}^3k \left[z+\mu - H_{\rm LDA}(\mathbf{k}) - \Sigma(z) \right]^{-1}_{\gamma_1\gamma_2}, \tag{2}$$

is calculated in a single-site approximation as given in [18]. Then, with the aid of the local Green's function $G(z)$, we evaluate the occupation matrix $n_{\gamma_1\gamma_2} = -\frac{1}{\pi}\,{\rm Im}\int_{-\infty}^{E_{\rm F}} {\rm d}z\,[G(z)]_{\gamma_1\gamma_2}$. The matrix $n_{\gamma_1\gamma_2}$ is used to construct an effective LDA+U potential V_U, which is inserted into Kohn–Sham-like equations:

$$[-\nabla^2 + V_{\rm LDA}(\mathbf{r}) + V_U + \xi(\mathbf{l}\cdot\mathbf{s})]\Phi^b_{\mathbf{k}}(\mathbf{r}) = \epsilon^b_{\mathbf{k}}\Phi^b_{\mathbf{k}}(\mathbf{r}). \tag{3}$$

These equations are iteratively solved until self-consistency over the charge density is reached. In each iteration, a new Green's function $G_{\rm LDA}(z)$ [which corresponds to $G(z)$ from Eq.(2) with the self-energy Σ set to zero] , and a new value of the $5f$-shell occupation are obtained from the solution of Eq. (3). Subsequently, a new self-energy $\Sigma(z)$ corresponding to the updated $5f$-shell occupation is constructed. Finally, the next iteration is started by evaluating the new local Green's function, Eq.(2).

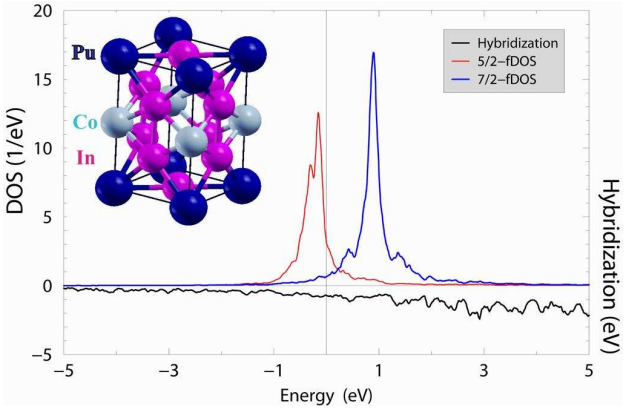

FIG. 1. (Color online) The Pu atom LDA $j = 5/2$, $7/2$ projected DOS, and LDA hybridization function $\Delta(\epsilon) = -\frac{1}{\pi} ImTr[G^{-1}(\epsilon+i\delta)]$. The inset shows the $PuCoIn_5$ crystal structure.

In order to determine the bath parameters V^k and ϵ^k, we assume that the LDA represents the non-interacting model. We then associate the LDA Green's function $G_{\rm LDA}(z)$ with the Hamiltonian of Eq. (1) when the coefficients of the Coulomb interaction matrix are set to zero ($U_{mm'm''m'''} = 0$). The hybridization function $\Delta(\epsilon)$ is then estimated as $\Delta(\epsilon) = -\frac{1}{\pi}\,{\rm Im\,Tr}[G^{-1}_{\rm LDA}(\epsilon + i\delta)]$. The curve obtained for $\Delta(\epsilon)$ is shown in Fig. 1, together with the $j = 5/2, 7/2$-projected LDA densities of the f-states. The results also show that the hybridization matrix is, to a good approximation, diagonal in the $\{j, j_z\}$ representation. Thus, we assume the first and fourth terms in the impurity model, Eq. (1), to be diagonal in $\{j, j_z\}$, so that we only need to specify one bath state (six orbitals) with $\epsilon^{k=1}_{j=5/2}$ and $V^{k=1}_{j=5/2}$, and another bath state (eight orbitals) with $\epsilon^{k=1}_{j=7/2}$ and $V^{k=1}_{j=7/2}$. Assuming that the most important hybridization is the one occurring in the vicinity of E_F, the numerical values of the bath parameters $V^{k=1}_{5/2,7/2}$ are found from the relation [20] $\sum_k |V^j_k|^2 \delta(\epsilon^j_k - \epsilon) = -\Delta(\epsilon)/N_f$ integrated over the

energy interval, $E_F - 0.5$ eV $\leq \epsilon \leq E_F + 0.5$ eV, with $N_f = 6$ for $j = 5/2$ and $N_f = 8$ for $j = 7/2$. The bath-state energies $\epsilon^{k=1}_{5/2,7/2}$ shown in Table I are adjusted to approximately reproduce the LDA $5f$-state occupations $n_f^{5/2}$ and $n_f^{7/2}$.

TABLE I. $5f$-states occupations $n_f^{5/2}$ and $n_f^{7/2}$, and bath state parameters $\epsilon^1_{5/2,7/2}$ (eV), $V^1_{5/2,7/2}$ (eV) for Pu-atom in $PuCoIn_5$, $PuCoGa_5$, and δ-Pu from LDA calculations.

Material	$n_f^{5/2}$	$n_f^{7/2}$	$\epsilon_1^{5/2}$	$V_1^{5/2}$	$\epsilon_1^{7/2}$	$V_1^{7/2}$
$PuCoIn_5$	4.78	0.39	0.36	0.21	-0.25	0.25
$PuCoGa_5$	4.38	0.76	0.25	0.29	-0.07	0.34
δ-Pu	4.16	0.85	0.33	0.27	-0.01	0.36

In the calculations we used an in-house implementation [21, 22] of the FP-LAPW method that includes both scalar-relativistic and spin-orbit coupling effects. The calculations were carried out assuming a paramagnetic state with crystal structure parameters for $PuCoIn_5$, $PuCoGa_5$, and δ-Pu taken from Refs. [11, 23, 24], respectively. The Slater integrals were chosen as $F_0 = 4.0$ eV, and $F_2 = 7.76$ eV, $F_4 = 5.05$ eV, and $F_6 = 3.07$ eV [25]. They corresponds to commonly accepted values for Coulomb's $U = 4.0$ eV and exchange $J = 0.64$ eV. The SOC parameters $\xi = 0.28$ eV for $PuCoIn_5$ and $PuCoGa_5$ and 0.29 eV for δ-Pu were determined from LDA calculations. CF effects were found to be negligible and $\Delta_{\rm CF}$ was set to zero. For the double-counting term entering the definition of the LDA+U potential, V_U, we have adopted the fully-localized (or atomic-like) limit (FLL) $V_{dc} = U(n_f - 1/2) - J(n_f - 1)/2$. Furthermore, we set the radii of the atomic spheres to 3.1 a.u. (Pu), 2.3 a.u. (Co), 2.3 a.u. (Ga), and 2.5 a.u. (In). The parameter $R_{Pu} \times K_{\rm max} = 10.54$ determined the basis set size, and the Brillouin zone (BZ) sampling was performed with 1152 k points. The self-consistent procedure defined by Eqs. (1)–(3) was repeated until the convergence of the $5f$-manifold occupation n_f was better than 0.01.

We are now ready to discuss the solution of Eq.(1). For $PuCoIn_5$, the ground state of the cluster formed by the $5f$ shell and the bath is given by a superposition of a magnetic sextet (23%) and a non-magnetic singlet (77%), with occupation numbers $\langle n_f \rangle = 5.40$ in the f shell and $\langle n_{bath} \rangle = 8.40$ in the bath states. This ground state is not a singlet and carries a nonzero magnetic moment. For the $5f$ shell alone, the expectation values of the spin (S_f), orbital (L_f) and total (J_f) angular moments can be calculated as $\langle \hat{X}_f^2 \rangle = X_f(X_f + 1)$ ($X_f = S_f, L_f, J_f$), giving $S_f = 2.27$, $L_f = 3.90$, and $J_f = 2.09$. The individual components of the moments vanish, $\langle \hat{S}_f^z \rangle = \langle \hat{L}_f^z \rangle = 0$, unless the symmetry is broken by an external magnetic field.

In the case of $PuCoGa_5$, on the other hand, the hybridized ground state of the impurity is a nonmagnetic singlet with all angular moments of the $5f$-bath cluster equal to zero ($S = L = J = 0$). It consists of $\langle n_f \rangle = 5.30$ f states and $\langle n_{bath} \rangle = 8.70$ bath states. In a pictorial way, we can imagine that the magnetic moment of the $5f$ shell (for which we get $S_f = 2.18$, $L_f = 4.05$, $J_f = 2.43$) is completely compensated by the moment carried by the electrons in the conduction band. As the value of the $5f$ magnetic moment fluctuates in time, because of the intermediate-valence electronic configuration, this compensation must be understood as dynamical in nature. The same situation is realized in δ-Pu ($S_f = 2.11$, $L_f = 4.21$, $J_f = 2.62$), whose ground state is found to be a nonmagnetic singlet with $\langle n_f \rangle = 5.21$ and $\langle n_{bath} \rangle = 8.79$.

The $5f$-orbital density of states (DOS) obtained from Eq. (2) for the three investigated compounds is shown in Fig. 2. Below the Fermi energy E_F the DOS exhibits the three-peak structure typical for Pu and for a number of its compounds, and its shape is in good agreement with experimental photoemission spectra. It can be noticed that the multiplets for the atomic f^6 configuration ($f^6 \rightarrow f^5$ transition, lying closer to E_F) are better resolved than for the f^5 part of the spectrum ($f^5 \rightarrow f^4$ transition).

Comparison with previous LDA+Hubbard-I (HIA) calculation for δ-Pu [18], and $PuCoGa_5$ [26] shows that the three-peak manifold lying above 2 eV binding energy has a slight upright shift towards E_F. At binding energies around 4 eV, the LDA+HIA peaks are substantially modified, and in the LDA+ED calculations they are spread over a ~ 3 eV energy interval. These changes in the DOS are induced by the hybridization and suggest partial delocalization of the f^5 multiplet. This is a situation suggested first by Hanzawa [27] in intermediate-valence rare-earth compounds such as SmS or SmB_6, where fluctuations occur between two atomic-like $4f$ configurations. Here, the $5f$ states remain localized for the f^6 configuration but become itinerant for the f^5 one.

As the many-body resonances lying closer to the Fermi energy are produced by $f^6 \rightarrow f^5$ multiplet transitions, they are in a way analogs to the *Racah* peaks, specific transitions between Racah multiplets [28] of f^n and $f^{n\pm1}$. On the other hand, these structures determine the metallic character of the investigated materials that can therefore be considered as a realization of a *Racah* metal, situated between the two limiting cases represented by fully localized intermediate-valence rare-earth compounds and metallic systems (e.g., nickel) with a non-integer number of d electrons.

Both $PuCoGa_5$ and δ-Pu display a temperature-independent magnetic susceptibility at low temperatures [6, 29]. Analogous to the intermediate-valence rare-earth compounds [30], the magnetic susceptibil-

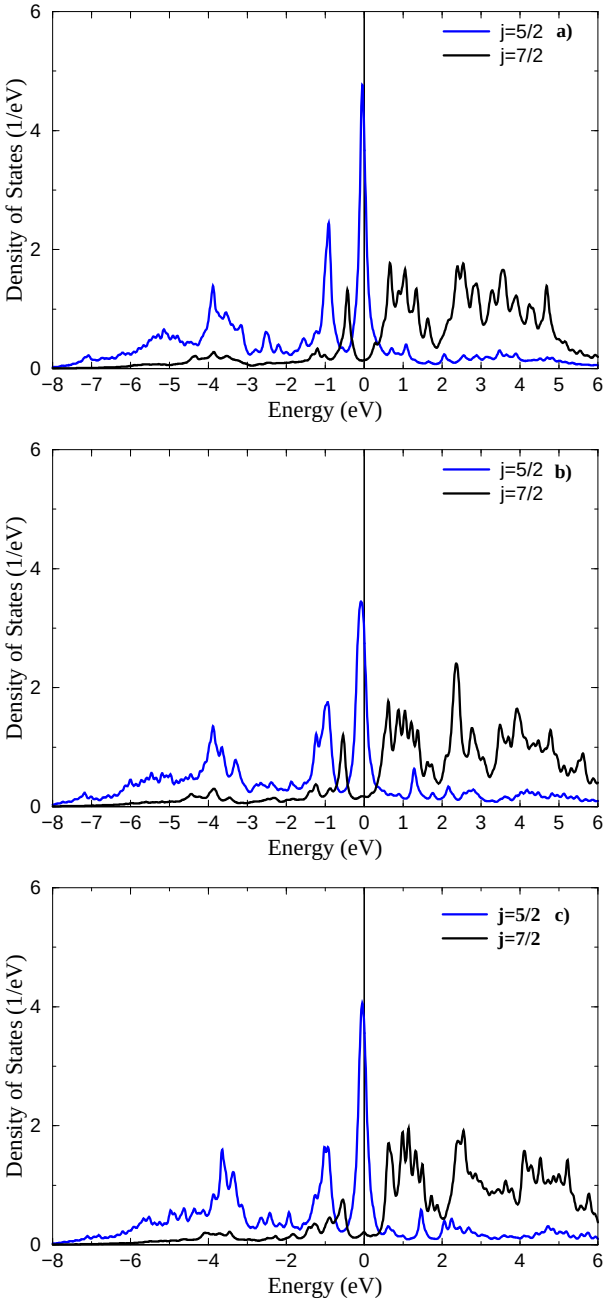

FIG. 2. (Color online) f-electron density of states (DOS, $j = 5/2$, $7/2$ projected) for the Pu atom in $PuCoIn_5$ (a), $PuCoGa_5$ (b) and δ-Pu (c).

ity is anticipated to behave as $\chi \sim 1/(T+T_{fc})$, where the temperature T_{fc} describes fluctuations between the $5f$ and conduction band electron states. T_{fc} corresponds indeed to the broadening of the quasiparticle resonance near E_F due to valence fluctuations [31]. As the ground state of the impurity is a singlet, we estimate T_{fc} using a renormalized perturbation theory of the Anderson model [16], $T_{fc} = -\frac{\pi^2}{4} Z[\Delta(E_F)/N_f]$, where $[\Delta(E_F)/N_f]$ is the hybridization per orbital at E_F, and Z is a quasiparticle weight, $Z = (\mathrm{Tr}[N(E_F)(1 - \frac{d\Sigma(\epsilon)}{d\epsilon})|_{\epsilon=E_F}]/\,\mathrm{Tr}[N(E_F)])^{-1}$. We get $T_{fc} = 72$ meV (~ 850 K) for $PuCoGa_5$ and $T_{fc} = 63$ meV (~ 750 K) for δ-Pu. Since T_{fc} is high, χ remains constant for $T \ll T_{fc}$, as observed experimentally for $PuCoGa_5$ and δ-Pu. The situation is different in the case of $PuCoIn_5$ where the ground state of the impurity is not a pure singlet due to weaker hybridization. Consequently, the temperature dependence of χ is expected to be more pronounced.

The electronic specific-heat coefficient can be estimated as $\gamma = \frac{\pi^2}{3} k_B^2\, \mathrm{Tr}[N(E_F)(1 - \frac{d\Sigma(\omega)}{d\omega})|_{\omega=0}]$. For δ-Pu, we get ≈ 44 mJ K^{-2} mol^{-1}, in very good agreement with experimental data. For $PuCoGa_5$, we get ≈ 43 mJ K^{-2} mol^{-1} which is smaller than the experimental value of 80–100 mJ K^{-2} mol^{-1}. For $PuCoIn_5$, the estimated γ value of ≈ 52 mJ K^{-2} mol^{-1} is even further away from the experimental value of ≈ 180 mJ K^{-2} mol^{-1}. In this case, it is difficult to obtain an accurate value for γ due to the sharp DOS peak in the vicinity of E_F (see Fig. 2). When taken right at the DOS peak position, the γ value of 95 mJ K^{-2} mol^{-1} is obtained. Also, note that a possible enhancement of

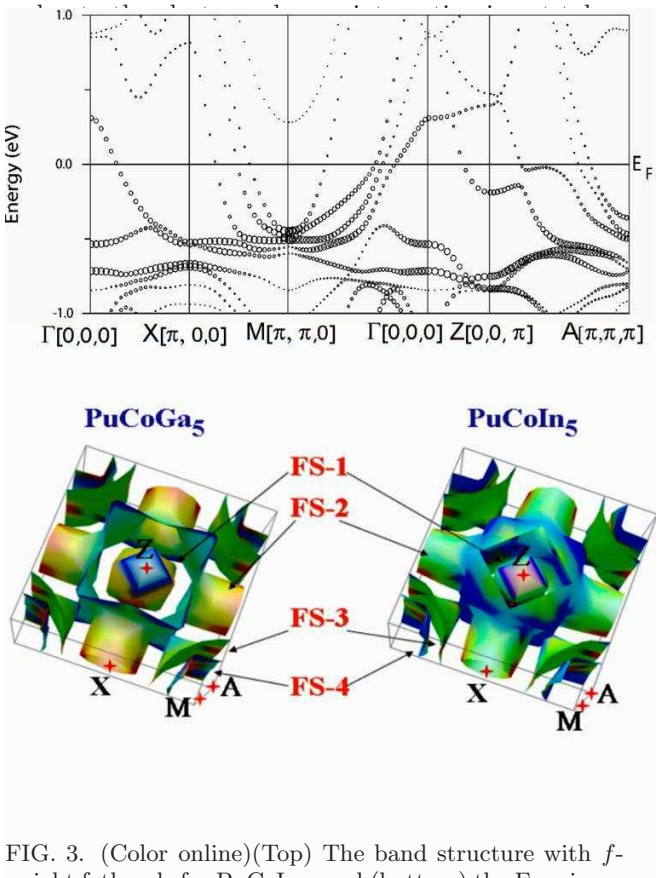

FIG. 3. (Color online)(Top) The band structure with f-weight fatbands for $PuCoIn_5$, and (bottom) the Fermi surface of $PuCoGa_5$ and $PuCoIn_5$ obtained from LDA+ED calculations. The shade of colors encodes the size of the energy gradient.

Figure 3 shows the band structure and the corre-

sponding Fermi Surface (FS) for $PuCoIn_5$, calculated from the solutions of Eq. (3), which represents an extended LDA+U static-mean-field band structure with the $5f$-states occupation matrix obtained from the local impurity Greens function Eq.(2). For comparison, Fig. 3 shows also the FS for $PuCoGa_5$ (Fig. S2 of Ref. [10]). Close similarities in the band structure of the two compounds are immediately apparent. Both are compensated multiband metals, as the Fe-based superconductors, and for both materials the f bands move away from the Fermi level when the Coulomb-U is included, as can be seen by examining the f-weighted fatbands. The Fermi surfaces are composed by four sheets (1–4), one that is hole-like (FS-1) and three that are electron-like (FS-2,3,4). The Fermi velocities ratio $\langle v_{x,y}^2\rangle^{\frac{1}{2}}/\langle v_z^2\rangle^{\frac{1}{2}}$ of 1.54 for $PuCoIn_5$, and 1.55 for $PuCoGa_5$ are calculated in reasonable agreement with the experimental anisotropy ratio of the critical field H_{c2}, $2-2.3$ for $PuCoIn_5$, and indicate a two-dimensional character of the electronic structure.

DFT electronic structure calculations for Pu-based 115 material have recently been reported by Ronning *et al.* [13] and Zhu *et al.* [12] Their analysis of the DFT band structure and FS (see, e.g., Figs. 3 and 4 of Ref. [12]) indicated two possible superconducting gap symmetries, the so-called $s\pm$ and $d_{x^2-y^2}$, which correspond to a pairing potential peaked at the $(\pi,\pi,0)$ reciprocal lattice position. The conclusion was drawn that for Pu-based "115" superconductors, the $s\pm$ order parameter is more likely that the $d_{x^2-y^2}$ one. This is in contradiction with point-contact spectroscopy results [10] showing a zero-bias conductance anomaly that is not expected for $s\pm$ gap symmetry [32].

The presence of a $5f$ local moment dynamically compensated by the surrounding conduction electrons together with the f^5-f^6 intermediate-valence ground state in $PuCoGa_5$ and $PuCoIn_5$ opens various possibilities for unconventional superconductivity. In $PuCoIn_5$ the Pu f-shell local moment is not fully compensated and superconductivity could be related to an antiferromagnetic quantum critical point [11, 33]. On the other hand, in $PuCoGa_5$ the ground state is a singlet and it seems more plausible that superconductivity results from a valence instability, as in heavy-fermion superconductors [34].

We are grateful to D. Daghero and L. Havela for helpful comments and discussion. We acknowledge financial support from Czech Republic Grants No. GACR P204/10/0330 and No. GAAV IAA100100912 and from DFG Grant No. 436 TSE 113/53/0-1.

[1] B. Johansson, Phys. Rev. B **11**, 2740 (1975).
[2] M. I. Katsnelson, I. V. Solovyev, and A. V. Trefilov, JETP Letters **56**, 272 (1992).
[3] S. Y. Savrasov, G. Kotliar, and E. Abrahams, Nature **410**, 793 (2001).
[4] A. Georges, G. Kotliar, W. Krauth, and M. Rozenberg, Rev. Mod. Phys. **68**, 13 (1996).
[5] J. H. Shim, K. Haule, and G. Kotliar, Nature **446**, 513 (2007).
[6] J. C. Lashley, A. Lawson, R. J. McQueeney, and G. H. Lander, Phys. Rev. B **72**, 054416 (2005).
[7] J. Sarrao *et al.*, Nature **420**, 297 (2002).
[8] N. J. Curro *et al.*, Nature **434**, 622 (2005).
[9] F. Jutier *et al.*, Phys. Rev. B **77**, 024521 (2008).
[10] D. Daghero *et al.*, Nat. Commun. **3**, 786 (2012).
[11] E. Bauer *et al.*, J. Phys. Condens. Matter **24**, 052206 (2012).
[12] J.-X. Zhu *et al.*, Europhys. Lett. **97**, 57001 (2012).
[13] F. Ronning *et al.*, J. Phys. Condens. Matter **24**, 294206 (2012).
[14] J. Rusz and P. M. Oppeneer, unpublished (2012).
[15] J. Kolorenč, A. I. Poteryaev, and A. I. Lichtenstein, Phys. Rev. B **85**, 235136 (2012).
[16] A. Hewson, *The Kondo Problem to Heavy Fermions* (Cambridge University Press, 1993).
[17] E. Wimmer, H. Krakauer, M. Weinert, and A. J. Freeman, Phys. Rev. B. **24**, 864 (1981).
[18] A. B. Shick, J. Kolorenč, A. I. Lichtenstein, and L. Havela, Phys. Rev. B **80**, 085106 (2009).
[19] A. I. Lichtenstein and M. I. Katsnelson, Phys. Rev. B **57**, 6884 (1998).
[20] O. Gunnarsson, O. K. Andersen, O. Jepsen, and J. Zaanen, Phys. Rev. B **39**, 1708 (1989).
[21] A. B. Shick, A. I. Liechtenstein, and W. E. Pickett, Phys. Rev. B **60**, 10763 (1999).
[22] A. B. Shick and W. E. Pickett, Phys. Rev. Lett. **86**, 300 (2001).
[23] I. Opahle and P. M. Oppeneer, Phys. Rev. Lett. **90**, 157001 (2003).
[24] H. M. Ledbetter and R. L. Moment, Acta Metall. **24**, 891 (1976).
[25] K. Moore and G. van der Laan, Rev. Mod. Phys. **81**, 235 (2009).
[26] A. B. Shick, J. Rusz, J. Kolorenč, P. M. Oppeneer, and L. Havela, Phys. Rev. B **83**, 155105 (2011).
[27] K. Hanzawa, J. Phys. Soc. Jpn. **67**, 3151 (1998).
[28] G. Racah, Phys. Rev. **76**, 1352 (1949).
[29] A. Hiess *et al.*, Phys. Rev. Lett. **100**, 076403 (2008).
[30] D. Khomskii, Sov. Phys. Usp. **129**, 443 (1979).
[31] C. M. Varma and Y. Yafet, Phys. Rev. B **13**, 2950 (1976).
[32] D. Daghero, M. Tortello, G. Ummarino, and R. Gonnelli, Rep. Prog. Phys. **74**, 124509 (2011).
[33] T. Das, J.-X. Zhu, and M. J. Graf, Phys. Rev. Lett. **108**, 017001 (2012).
[34] K. Miyake, J. Phys. Condens. Matter **19**, 125201 (2007).